Acta Crystallographica Section D
Biological Crystallography
ISSN 1399-0047

Structural basis for DNA-mediated allosteric regulation facilitated by the AAA$^+$ module of Lon protease

Alan Yueh-Luen Lee,[a]‡ Yu-Da Chen,[b,c]‡ Yu-Yung Chang,[b]‡ Yu-Ching Lin,[d] Chi-Fon Chang,[e] Shing-Jong Huang,[f] Shih-Hsiung Wu[c,d]* and Chun-Hua Hsu[b,g,h]*

[a]National Institute of Cancer Research, National Health Research Institutes, Zhunan, Miaoli 35053, Taiwan, [b]Department of Agricultural Chemistry, National Taiwan University, Taipei 10617, Taiwan, [c]Institute of Biochemical Sciences, National Taiwan University, Taipei 10617, Taiwan, [d]Institute of Biological Chemistry, Academia Sinica, Taipei 11529, Taiwan, [e]Genomics Research Center, Academia Sinica, Taipei 11529, Taiwan, [f]Instrumentation Center, National Taiwan University, Taipei 10617, Taiwan, [g]Genome and Systems Biology Degree Program, National Taiwan University, Taipei 10617, Taiwan, and [h]Center for Systems Biology, National Taiwan University, Taipei 10617, Taiwan

‡ A-YL, Y-DC and Y-YC made equal contributions to this manuscript and can be considered co-first authors.

Correspondence e-mail: shwu@gate.sinica.edu.tw, andyhsu@ntu.edu.tw

Received 31 May 2013
Accepted 23 September 2013

PDB reference: α subdomain of Bt-Lon, 4git

Lon belongs to a unique group of AAA$^+$ proteases that bind DNA. However, the DNA-mediated regulation of Lon remains elusive. Here, the crystal structure of the α subdomain of the Lon protease from *Brevibacillus thermoruber* (Bt-Lon) is presented, together with biochemical data, and the DNA-binding mode is delineated, showing that Arg518, Arg557 and Arg566 play a crucial role in DNA binding. Electrostatic interactions contributed by arginine residues in the AAA$^+$ module are suggested to be important to DNA binding and allosteric regulation of enzymatic activities. Intriguingly, Arg557, which directly binds DNA in the α subdomain, has a dual role in the negative regulation of ATPase stimulation by DNA and in the domain–domain communication in allosteric regulation of Bt-Lon by substrate. In conclusion, structural and biochemical evidence is provided to show that electrostatic interaction in the AAA$^+$ module is important for DNA binding by Lon and allosteric regulation of its enzymatic activities by DNA and substrate.

1. Introduction

Lon is a highly conserved ATP-dependent protease that is present in archaea and prokaryotes, as well as in eukaryotic mitochondria (Chung & Goldberg, 1981; Fukui *et al.*, 2002; van Dyck *et al.*, 1994; Wang *et al.*, 1993). It plays an important role in intracellular protein degradation (Goldberg *et al.*, 1994; Gottesman & Maurizi, 1992; Maurizi, 1992) and selectively degrades damaged and abnormal proteins and several short-lived transcription factors that control cell division, the synthesis of capsular oligosaccharides, pathogenesis and the formation of biofilms (Gottesman, 1996; Robertson *et al.*, 2000; Takaya *et al.*, 2002; Zhu & Winans, 2001). Monomeric Lon is a single polypeptide consisting of an N-terminal domain, a central ATPase domain (also called the AAA$^+$ module), which contains a large α/β subdomain and a small α subdomain [also called the sensor and substrate-discrimination (SSD) domain], and a C-terminal protease domain (Botos *et al.*, 2004; Rotanova *et al.*, 2006; Roudiak & Shrader, 1998; Vasilyeva *et al.*, 2002). Lon has been proposed to be a member of the AAA$^+$ superfamily, a class of chaperone-like ATPases that assist in the assembly, operation and disassembly of protein–DNA complexes (Neuwald *et al.*, 1999). Furthermore, Lon has now been shown to exhibit chaperone-like activity (Cheng *et al.*, 2013; Lee, Hsu *et al.*, 2004; Lee, Tsay *et al.*, 2004), suggesting that it may function as a DNA–protein complex 'molecular matchmaker', a class of proteins that use the energy released by ATP hydrolysis to cause a conformational change in one or both components of a DNA-binding protein pair (Sancar & Hearst, 1993).

Lon is a DNA-binding protein (Fu & Markovitz, 1998; Fu *et al.*, 1997; Lee, Hsu *et al.*, 2004; Zehnbauer *et al.*, 1981). Although its DNA-binding activity has been predicted to be crucial to its physiological function on the basis of studies of other DNA-binding proteases (Gillette *et al.*, 2004; Gonzalez *et al.*, 2002; He *et al.*, 1995; Zheng & Johnston, 1998), the effects of DNA binding on the physiological functions of Lon are not clearly understood. Previous studies have shown that Lon is involved in gene expression or genome stability in prokaryotes (Gill *et al.*, 1993; Mizusawa & Gottesman, 1983; Schmidt *et al.*, 1994; Takaya *et al.*, 2002) and in the mitochondria of eukaryotes (Alexandre *et al.*, 2007; Chen *et al.*, 2008; Suzuki *et al.*, 1994; Van Dyck *et al.*, 1994, 1998). Recent reports have further suggested that Lon is a component of mitochondrial nucleoids in human mitochondria, where it degrades or processes proteins involved in DNA metabolism and replication (Alexandre *et al.*, 2007; Liu *et al.*, 2004). Lon is classified as a DNA-binding protein with low specificity (Charette *et al.*, 1984; Chung & Goldberg, 1982; Zehnbauer *et al.*, 1981) and it binds nonspecifically to plasmid DNA (Charette *et al.*, 1984; Chung & Goldberg, 1982; Zehnbauer *et al.*, 1981) or chromosomal DNA (Charette *et al.*, 1984; Nomura *et al.*, 2004).

Lon is an ATP-dependent allosteric enzyme, the activities of which are regulated by DNA and its protein substrates. The roles of the protein substrate in the allosteric regulation of Lon activity have been studied; in *Escherichia coli* Lon the substrate stimulates ATP-dependent proteolysis by promoting ATP binding and the release of bound ADP (Lee & Suzuki, 2008; Menon & Goldberg, 1987). The binding and hydrolysis of the protein substrate and the ATP binding and hydrolysis/ADP dissociation/ATP rebinding cycle induce conformational changes in *E. coli* Lon (Licht & Lee, 2008; Menon & Goldberg, 1987; Patterson *et al.*, 2004; Vasilyeva *et al.*, 2002). However, the effects of DNA binding on Lon activity are controversial. Chung & Goldberg (1982) reported that DNA binding to *E. coli* Lon stimulates its ATP-dependent protease activity and that this is dependent on the concentration of the DNA and protein substrates. Charette *et al.* (1984) reported that a high concentration of DNA significantly inhibits *E. coli* Lon protease activity, but that this inhibition can be prevented by increasing the protein substrate concentration. Sonezaki *et al.* (1995) also showed that the binding of *E. coli* Lon to plasmid DNA is reduced by high concentrations of unfolded protein substrates or heat shock. Conversely, Liu *et al.* (2004) reported that the DNA-binding affinity of human mitochondrial Lon protein is increased by substrate and is inhibited by ATP. They also proposed that Lon undergoes different conformational changes induced by protein substrate and ATP that are required to effect DNA binding. Accordingly, little is known about the allosteric regulation by DNA binding that affects the enzymatic activities of Lon.

We previously demonstrated that Lon from *Brevibacillus thermoruber* (Bt-Lon) is a DNA-binding protein and that the α subdomain of the protease is involved in DNA binding (Lee, Hsu *et al.*, 2004; Lee, Tsay *et al.*, 2004). With the aim of elucidating the DNA-recognition mode of Bt-Lon, protein crystallography and NMR techniques were employed to determine the structures of free and DNA-bound forms of the α subdomain. The crystal structure of the α subdomain shows a continuous surface with highly positively charged residues such as arginine. An information-driven docking model of the α subdomain–DNA complex also implies that electrostatic forces mediate the interactions between Bt-Lon and DNA. Based on the structural analysis, biochemical studies were performed to demonstrate that electrostatic interaction plays important roles in the DNA-binding properties of the α subdomain of Bt-Lon and domain–domain interaction *via* conformational changes in the AAA^+ module in substrate-mediated allosteric stimulation. Furthermore, the effect of various concentrations of DNA on regulation of the enzymatic activities and oligomeric status of Bt-Lon was investigated.

2. Materials and methods

2.1. Enzymes and chemicals

Restriction enzymes were purchased from New England Biolabs (London, England). The fluorogenic peptide glutaryl-Ala-Ala-Phe-methoxynaphthylamide (Glt-AAF-MNA) was purchased from Bachem (Bubendorf, Switzerland). Dithiothreitol (DTT) and glutaraldehyde were purchased from Sigma (St Louis, USA).

2.2. Protein production

Full-length Bt-Lon and its mutants were overexpressed in *E. coli* strain BL21(DE3) (Novagen) and purified as described previously (Lee, Hsu *et al.*, 2004; Lee, Tsay *et al.*, 2004). For X-ray and NMR studies, residues 491–605 of Bt-Lon, comprising the α subdomain with an extra Met residue at the N-terminus and LEHHHHHH tag residues at the C-terminus, was overexpressed from pET-21a vector (Novagen) in *E. coli* strain BL21(DE3). The cells were grown in Luria–Bertani medium or MOPS medium supplemented with $^{15}NH_4Cl$ and/or ^{13}C-glucose at 37°C; ampicillin (50 µg ml^{-1}) was added for plasmid selection. The medium was inoculated (1:20) with an overnight culture and incubated until the culture reached an OD_{600} of 0.6. Protein expression was induced by the addition of 1.0 m*M* isopropyl β-D-1-thiogalactopyranoside to the medium. The cells were harvested by centrifugation after 3 h and resuspended in buffer consisting of 50 m*M* sodium phosphate pH 8.0, 300 m*M* NaCl, 5% glycerol. Clarified lysates were applied onto nickel-affinity columns (Qiagen, Hilden, Germany) to obtain protein of up to 90% purity as judged by SDS–PAGE. Protein fractions were subjected to gel-filtration chromatography using a Superdex 75 XK 16/60 column (Amersham Biosciences) equilibrated with buffer consisting of 50 m*M* sodium phosphate pH 7.0 with 100 m*M* NaCl and eluted at a flow rate of 0.8 ml min^{-1}. The purity of the eluted protein on Coomassie Blue-stained SDS–PAGE was shown to be greater than 95%. The protein concentration of the purified protein was determined by the Bradford method (Bradford, 1976) using bovine serum albumin as a standard.

2.3. Crystal structure determination

The duplex nucleotide sequence 5′-CTGTTAGCGGGC-3′ (ds-ms1) was previously identified as a Bt-Lon α subdomain binding motif by MALDI–TOF mass spectroscopy and a DNase I protection assay (Lin *et al.*, 2009). A crystal form was obtained during attempts to crystallize a Bt-Lon α subdomain–DNA complex. Protein solution (6.7 mg ml^{-1}) was mixed in a 1:1.2 ratio with the 12-mer duplex DNA (ds-ms1) and adjusted with 0.7 *M* NaCl to prevent heavy precipitation. The final sample was dialysed against buffer consisting of 20 m*M* Tris–HCl pH 8.0, 250 m*M* NaCl, 5 m*M* DTT. Crystals was obtained in 0.1 *M* phosphate buffer pH 6.6, 0.2 *M* NaCl, 12.5% PEG 8000. The crystals grew at 10°C within one week using the sitting-drop vapour-diffusion method and belonged to space group *P*23, with unit-cell parameters $a = b = c = 93.8$ Å, $\alpha = \beta = \gamma = 90^\circ$ (Chen, Chang *et al.*, 2013). The crystals were flash-cooled in liquid nitrogen using mother liquor plus 20% glycerol as a cryoprotectant. Diffraction data were collected to 2.88 Å resolution on beamlines 13B1 and 13C1 at the National Synchrotron Radiation Research Center (NSRRC). The data were integrated and reduced using the *HKL*-2000 package (Otwinowski & Minor, 1997). This crystal form was readily solved by molecular replacement (MR) using a homology search model generated by *MODELLER* (Eswar *et al.*, 2008) from the *Bacillus subtilis* Lon protease structure (PDB entry 3m6a; Duman & Löwe, 2010). The initial MR solution was obtained using *Phaser* (McCoy *et al.*, 2007), which suggested the presence of two molecules in the asymmetric unit, but there was no evidence of bound DNA. Structure refinement was carried out by rounds of energy minimization and *B*-factor refinement using the *CNS* package (Brünger *et al.*, 1998). Manual model rebuilding was performed with *Coot* (Emsley & Cowtan, 2004) using composite OMIT maps generated by *CNS*. Final cycles of restrained refinement were performed using *REFMAC* (Murshudov *et al.*, 2011) and *PHENIX* (Adams *et al.*, 2010). The final model presents excellent geometry, with the Ramachandran analysis by *PROCHECK* (Morris *et al.*, 1992) indicating that 88.4 and 11.6% of the residues lie in the most favoured and the allowed regions, respectively (Table 1). All figures were produced with *PyMOL* (v.1.3r1; Schrödinger).

2.4. NMR and backbone resonance assignments

All NMR spectra were acquired at 298 and 310 K using a Bruker AVANCE 600 equipped with a QXI (^{1}H, ^{13}C, ^{15}N and ^{31}P) probe or an AVANCE 800 equipped with a *z*-gradient TXI (^{1}H, ^{13}C and ^{15}N) cryoprobe (Bruker, Karlsruhe, Germany). The sample (0.3 m*M* protein in 0.35 ml) was prepared in 50 m*M* sodium phosphate pH 6.5 containing 100 m*M* NaCl and 5 m*M* DTT in 90% H_2O/10% D_2O in a Shigemi (Allison Park, Pennsylvania, USA) NMR tube. All heteronuclear NMR spectra of the Bt-Lon α subdomain were obtained as described previously (Hsu *et al.*, 2003; Hsu & Wang, 2011). Assignment of the main-chain ^{1}N, $^1H^N$, $^{13}C^\alpha$, $^{13}C^\beta$ and $^{13}C'$ chemical shifts was based on HNCACB, CBCA(CO)NH, HNCO and HN(CA)CO spectra (Chen, Wu *et al.*, 2013). 4,4-Dimethyl-4-silapentane-1-sulfonate (DSS) was used as an external chemical shift standard at 0.00 p.p.m. The ^{15}N and ^{13}C chemical shifts were indirectly referenced using the consensus Ξ ratios of the zero-point frequencies at 310 K (Wishart *et al.*, 1995). All spectra were processed using the *NMRPipe* software package (Delaglio *et al.*, 1995) and were analyzed using *NMRView* (Delaglio *et al.*, 1995). Linear prediction was used in the ^{13}C and ^{15}N dimensions to improve the digital resolution.

Table 1
Data-collection and refinement statistics for the Bt-Lon α subdomain.

Values in parentheses are for the highest resolution shell.

Data-collection statistics	
Beamline	13C, NSRRC
Wavelength (Å)	0.975
Space group	*P*23
Unit-cell parameters (Å)	$a = b = c = 94.28$
Resolution range (Å)	29.82–2.88 (2.98–2.88)
Total observations	139259
Unique observations	6542 (641)
Completeness (%)	99.8 (100.0)
R_{merge} (%)	6.6 (50.4)
Average $I/\sigma(I)$	38.0 (9.0)
Refinement statistics†	
Reflections	6439
R_{work}/R_{free} (%)	20.1/24.8
R.m.s.d. from ideal geometry	
Bonds (Å)	0.009
Angles (°)	1.32
Ramachandran data‡, residues in (%)	
Most favoured regions	88.4
Allowed regions	11.6
Generously allowed regions	0
Disallowed regions	0

† All positive reflections were used in the refinement. ‡ Calculated using *PROCHECK*.

2.5. Protein–DNA interactions monitored by NMR

The 12-mer duplex DNA ds-ms1 (5′-CTGTTAGCGGGC-3′) and its analogue ds-ms2 (5′-CCGCTGGTGAGT-3′) were used for binding studies. The DNA was annealed by mixing equal aliquots of two oligomers, heating to 85°C and slow cooling to room temperature. The annealed DNA was checked on a 20% polyacrylamide gel visualized by ethidium bromide staining. For protein–DNA NMR studies, 0.1 m*M* ^{15}N-labelled Bt-Lon α subdomain in 50 m*M* sodium phosphate pH 6.5 with 5 m*M* DTT in 10% D_2O was titrated with 0.5, 1 and 1.5 molar equivalents of oligonucleotide, respectively, and the ^{1}H–^{15}N HSQC spectra were used to monitor protein chemical shift changes. The combined ^{1}H and ^{15}N chemical shift differences were calculated using the equation Δp.p.m. = $[(\Delta\delta H_N)^2 + (0.2\Delta\delta N)^2]^{1/2}$, in which 0.2 is the scaling factor for normalizing the ^{1}H and ^{15}N chemical shifts.

2.6. Molecular docking

A model of the Bt-Lon α subdomain–DNA complex was calculated using the information-driven method *HADDOCK* v.2.0 (Dominguez *et al.*, 2003; van Dijk *et al.*, 2006). Chemical shift perturbations (CSP) and DNA-specificity data were translated into ambiguous interaction restraints (AIRs) to

drive the docking process. The starting structures for the docking were a B-form model of the 12 bp ds-ms2 DNA duplex built by *Discovery Studio* 2.0 (Accelrys) and the crystal structure of the α subdomain. For the α subdomain protein, residues having a weighted chemical shift perturbation upon complex formation of greater than 0.05 p.p.m. and displaying high solvent accessibility (>50%) were selected as active residues. The solvent accessibility of the active residues was calculated using *NACCESS* (Hubbard & Thornton, 1993). The selected active residues of the protein were Met511, His514, Gly517, Val541, Glu547, Arg553, Lys554, Arg557, Val560, Arg566, Val567, Thr570, Thr573, Val574 and Glu575. The selected active DNA residues were 3′-CGGG and the four complementary nucleotides of the 12-mer dsDNA molecular model, since this specific DNA-binding sequence has been identified in a previous report (Lin *et al.*, 2009). During rigid-body energy minimization, 1000 structures were calculated and the 200 best solutions based on the intermolecular energy were used for semi-flexible simulated annealing followed by explicit water refinement. Docked structures corresponding to the 200 best solutions with the lowest intermolecular energies were generated. The 200 solutions were clustered using a 3.5 Å r.m.s.d. cutoff criterion. The clusters were ranked based on the averaged *HADDOCK* score of their top ten structures.

2.7. DAPI fluorimetric dye displacement assay

DAPI (4′,6′-diamidino-2-phenylindole; Molecular Probes) increases in fluorescence upon binding to the minor groove of double-stranded DNA. The standard reaction buffer consisted of 20 m*M* Tris pH 7.5, 10 m*M* $MgCl_2$, 400 n*M* DAPI (400 µl total volume), 6 µ*M* nucleotides and a variable amount of Bt-Lon α subdomain. Fluorescence measurements were performed on a Jasco luminescence spectrometer. The excitation and emission wavelengths were 345 and 467 nm and the slit widths were 5 and 10 nm, respectively. The reaction components were added as follows. After equilibration of the standard buffer at 20°C any background signal owing to buffer components was set to zero. The pET-28a plasmid DNA was added and the resulting fluorescence increased severalfold owing to the formation of the DAPI–DNA complex. Proteins were then added and the decrease in fluorescence of the DAPI–DNA complex was monitored after a 10 min incubation period. Relative fluorescence values were corrected for dilution effects and the subtraction of fluorescence arising from the buffer and DNA components.

2.8. Site-directed mutagenesis

Bt-Lon mutants were generated by site-directed mutagenesis using PCR and a previously constructed plasmid consisting of the Bt-Lon gene inserted into the pET-21a vector (Novagen) as a template (Lee, Tsay *et al.*, 2004). Two complementary primers containing the desired mutation sequence were used to convert Arg98, Arg370, Arg518, Arg557, Arg566, Arg590 or Arg697 to alanine. For each mutant, two separate PCRs were performed: one using the forward mutant primer, the corresponding Bt-Lon gene-specific primer flanked by *Xho*I sites and plasmid DNA with an insert coding for wild-type Bt-Lon and the other using the reverse mutant primer, the Bt-Lon gene-specific primer flanked by *Nde*I sites and the same plasmid DNA (Lee, Tsay *et al.*, 2004). The two PCR products were combined as templates in a new PCR containing both flanking primers for the first three cycles; an additional 5 units of *Taq* DNA polymerase (Promega) was added for the next 30 cycles. The final PCR product for each mutant was purified using a QIAquick PCR Purification Kit (Qiagen) and subcloned between the *Nde*I and *Xho*I sites of pET-21a. Each mutant plasmid was confirmed by DNA sequencing.

2.9. Peptidase and protease assays

The peptidase activity of Bt-Lon and its mutants was determined as described previously (Lee, Tsay *et al.*, 2004). In brief, the mixture for peptidase assays consisted of 50 m*M* Tris–HCl pH 8.0, 150 m*M* NaCl, 10 m*M* $MgCl_2$, 1.0 m*M* ATP, 0.3 m*M* Glt-AAF-MNA and 4 µg protein in a total volume of 200 µl. The reaction was carried out for 60 min at 50°C and was stopped by the addition of 100 µl 1% SDS and 1.2 ml 0.1 *M* sodium borate pH 9.2. Fluorescence was measured using a Hitachi F4010 fluorescence spectrophotometer with excitation at 335 nm and emission at 410 nm.

The mixture for protease assays consisted of 10 m*M* $MgCl_2$, 1.0 m*M* ATP, 50 m*M* Tris–HCl pH 8.0, 150 m*M* NaCl, 4.0 µg Bt-Lon, 10 µg α-casein fluorescein isothiocyanate type I (FITC-casein; Sigma) in a total volume of 200 µl (Twining, 1984). The reaction was carried out for 60 min at 323 K and was terminated by the addition of 10 µl 10 mg ml^{-1} bovine serum albumin (Sigma) and 100 µl 10% trichloroacetic acid. The mixtures were incubated for 10 min on ice and centrifuged for 10 min at 16 000*g* at 4°C; the supernatants were then transferred into fresh tubes and 200 µl 0.5 *M* CHES–Na pH 12.0 (Sigma) was added. The fluorescence was measured using a Hitachi F4010 fluorescence spectrophotometer with excitation at 490 nm and emission at 525 nm.

2.10. ATPase assays

ATPase assays were performed using the method of Lanzetta and coworkers for the detection of free inorganic phosphate (Lanzetta *et al.*, 1979). The reaction mixtures consisted of 50 m*M* Tris–HCl pH 8.0, 150 m*M* NaCl, 10 m*M* $MgCl_2$, 1.0 m*M* ATP and 4 µg Bt-Lon in a total volume of 200 µl and were incubated for 60 min at 50°C. Colour development was initiated by the addition of 800 µl malachite–molybdate solution and was terminated by the addition of 100 µl 34% sodium citrate. The optical density of the reaction mixture was measured at 660 nm and converted to phosphate concentration using K_2HPO_4 standards. One unit of ATPase activity was defined as the amount of enzyme required to release 1 nmol of inorganic phosphate per hour. Background hydrolysis values were subtracted in each assay.

2.11. Electrophoretic mobility-shift assay (EMSA)

For mobility-shift assays, 500 ng plasmid DNA (pET-21a) in 50 m*M* Tris–HCl pH 8.0, 150 m*M* NaCl, 10 m*M* $MgCl_2$ was incubated with 4 µg Bt-Lon and its mutants in a total volume of 25 µl for 30 min at 25°C and the protein–DNA complexes were then analyzed by electrophoresis on 0.8% agarose gels. DNA bands were visualized by ethidium bromide staining.

2.12. Circular-dichroism spectroscopy

Circular-dichroism spectra were recorded on a Jasco J-810 spectropolarimeter with a 0.1 cm light path for far-UV CD measurements at 25°C using 4 m*M* protein in 50 m*M* Tris–HCl pH 8.0, 10 m*M* $MgCl_2$, 150 m*M* NaCl. The bandwidth was 1.0 nm and the ellipticity measurements were averaged for 3 s at each wavelength. All spectra reported are the average of five scans.

The temperature dependence of the CD ellipticity at 222 nm was monitored using a 0.1 cm path-length cuvette using a Jasco J-810 spectropolarimeter equipped with a temperature controller (model RTE-111; Nealab, Portsmouth, New Hampshire, USA). The temperature of the protein solution (4 m*M*) was raised from 20 to 90°C at a rate of 60°C h^{-1}. The fractional amount of native protein was determined as $(\varepsilon - \varepsilon_D)/(\varepsilon_N - \varepsilon_D)$, where ε is the observed ellipticity and ε_N and ε_D are the ellipticity of the fully native and fully denatured proteins, respectively. The temperature parameter T_m was derived from the CD denaturation curve on the basis of a two-state mechanism (Pace, 1990).

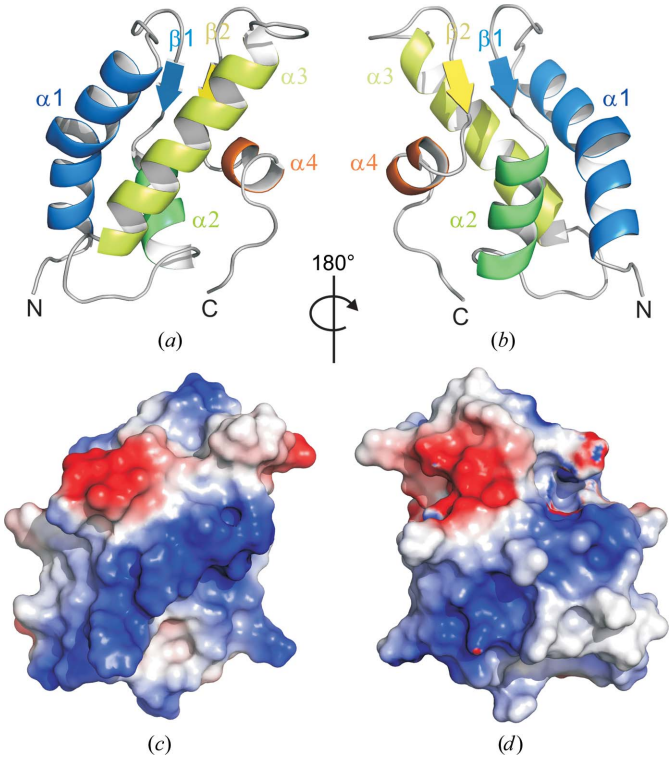

Figure 1
Overall structure and surface electrostatic features of the Bt-Lon α subdomain. (*a*) Ribbon representation of the crystal structure of the α subdomain. The protein secondary structure is labelled along the sequence and is rainbow-coloured with the N-terminus in blue and the C-terminus in orange. (*b*) The same cartoon after a 90° rotation around the vertical axis. (*c*, *d*) Surface-charge representations in the same orientations as (*a*) and (*b*), respectively, coloured according to the electrostatic surface potential. Basic, acidic and uncharged surface regions are coloured blue, red and white, respectively.

2.13. Tryptophan fluorescence measurements

Since Bt-Lon contains three Trp residues (Trp302, Trp602 and Trp651), the intrinsic Trp fluorescence spectrum could be used to estimate the binding affinity or monitor the conformational change of protein bound to DNA. The intensity of the fluorescence decreases as the polarity of the solvent surrounding the Trp residue increases (Ladokhin, 2000; Royer, 1995). The extent to which the fluorescence of a protein is quenched by DNA is proportional to the ratio of the binding affinity for DNA to the concentration of DNA (Royer, 1995). The fluorescence spectrum of 0.2 mg ml^{-1} Bt-Lon or its mutants in 50 m*M* Tris–HCl pH 8.0, 10 m*M* $MgCl_2$, 150 m*M* NaCl at 25°C was recorded in the presence or absence of allosteric regulators using an F-4500 fluorescence spectrophotometer (Hitachi, Japan); the emission spectrum was recorded from 300 to 400 nm with excitation at 295 nm.

3. Results

3.1. Crystal structure and DNA-binding model of the Bt-Lon α subdomain

Recently, we demonstrated that Bt-Lon is a DNA-binding protein and that the α subdomain of Bt-Lon is responsible for its DNA-binding ability (Lee, Hsu *et al.*, 2004; Lee, Tsay *et al.*, 2004). In addition, the duplex nucleotide sequence has been identified as the Bt-Lon α subdomain binding motif by DNase I protection assays and MALDI–TOF mass spectrometry (Lin *et al.*, 2009). We then crystallized the Bt-Lon α subdomain in complex with DNA and obtained a crystallization condition consisting of 0.1 *M* phosphate buffer pH 6.6, 0.2 *M* NaCl, 12.5% PEG 8000. The crystal structure of the Bt-Lon α subdomain was determined by molecular replacement using a homology model derived from the crystal structure of *B. subtilis* Lon protease (PDB entry 3m6a; Duman & Löwe, 2010). However, only the protein molecule was found in the crystal. Since the crystals of the Bt-Lon α subdomain had the same space group and similar unit-cell parameters and crystallization conditions in both the presence and the absence of DNA, we assume that the ionic strength of this condition may reduce the association between the protein and the DNA.

The solved structure was refined to yield a model (Supplementary Fig. S1[1]) with all residues in favourable regions of the Ramachandran plot (Supplementary Fig. S2) and an R_{work} of 20.1%. The structure factors and coordinates have been deposited in the Protein Data Bank as PDB entry 4git. The diffraction parameters and refinement statistics are shown in Table 1. The protein crystallized with *P*23 symmetry.

[1] Supporting information has been deposited in the IUCr electronic archive (Reference: YT5057).

Each asymmetric unit consisted of two Bt-Lon α subdomains with practically identical structures (r.m.s.d. of 0.153 Å). The Bt-Lon α subdomain contains four α-helices (α1, Glu495–His514; α2, Glu525–Gln534; α3, Arg542–Ile559; α4, Lys572–

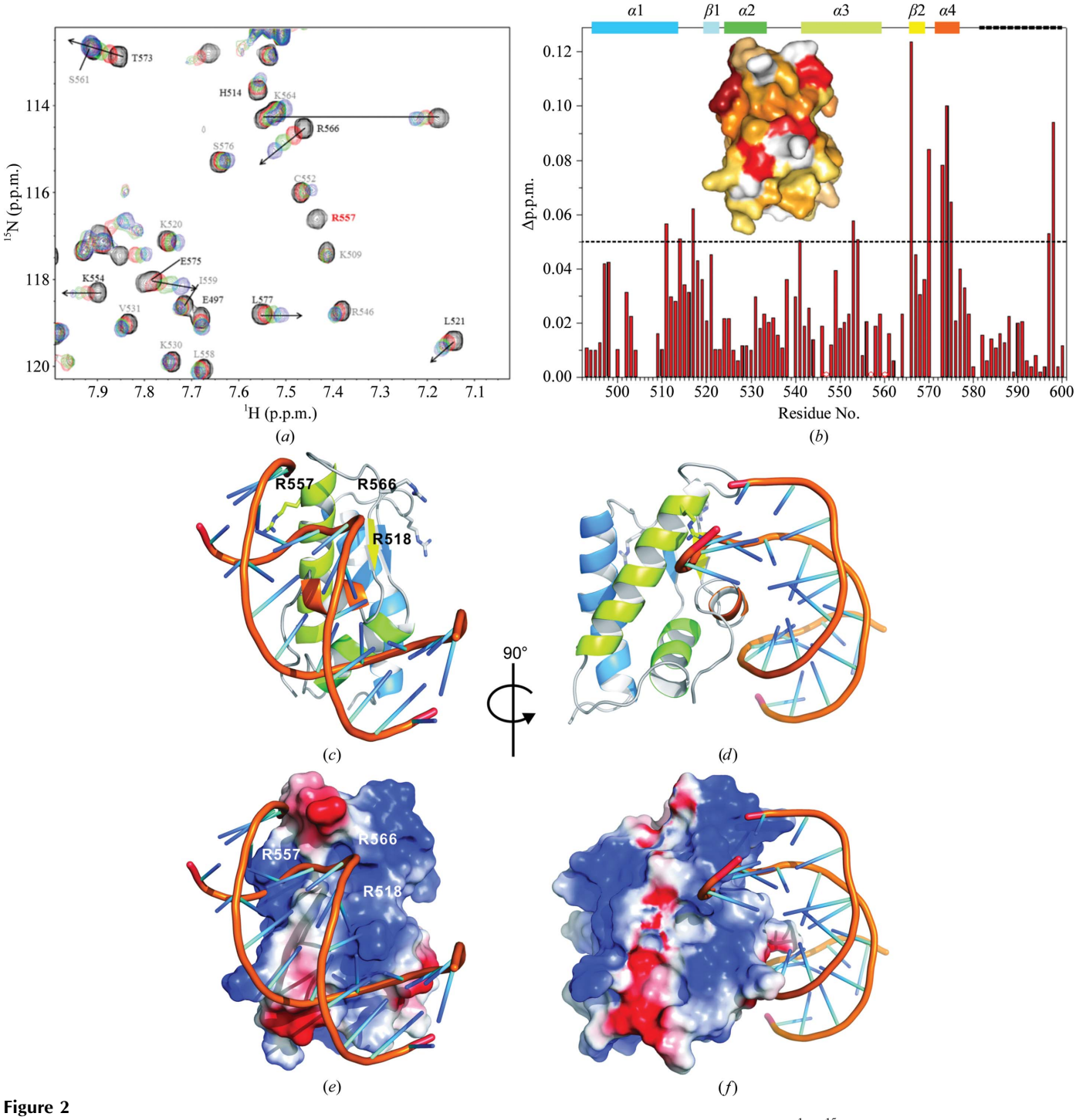

Figure 2

Mapping and docking of the DNA-binding region of the Bt-Lon α subdomain. (*a*) A selected region of the ^{1}H–^{15}N HSQC spectrum shows free α subdomain (black) titrated with 0.5 (red), 1 (green) and 1.5 (blue) molar equivalents of ds-ms2 DNA. The residues exhibiting significant shift changes or disappearing after DNA titration are labelled with assignment annotation. (*b*) The normalized chemical shift changes induced by binding of ds-ms2. The assigned secondary-structure regions are shown at the top and residues with chemical shift changes larger than 0.05 p.p.m. are labelled. The inset figure shown in the same orientation in (*c*) and (*e*) indicates the mapping of the duplex DNA interacting with the α subdomain surface. The chemical shift changes are coloured from red to yellow for large to small. (*c*, *d*) Schematic representation of the *HADDOCK* model of the Bt-Lon α subdomain in complex with ds-ms2 in two orientations. Secondary structures are represented by coloured ribbons. The two strands of DNA backbone and bases are represented by orange-coloured and green-coloured ropes and bases, respectively. (*e*, *f*) Surface-charge representations of the Bt-Lon α subdomain–ds-ms2 DNA complex in two orientations to highlight the arrangement of the positively charged residues and the DNA backbone. Positively charged surface is coloured blue and negatively charged surface is coloured red.

Table 2
Statistics of the top seven clusters obtained with *HADDOCK*.

Cluster†	*HADDOCK* score‡	R.m.s.d., E_{min}§	*N*¶	E_{vdw}††	E_{elec}††	E_{AIR}‡‡	BSA§§	E_{desolv}¶¶	*Z*-score†††
1	−77.1 ± 10.5	0.9 ± 0.5	16	−52.5 ± 7.7	−491.4 ± 22.0	507.3 ± 51.1	1680.9 ± 90.8	23.0 ± 4.4	−1.8
10	−67.7 ± 5.2	11.5 ± 0.2	4	−55.6 ± 5.0	−442.5 ± 65.5	537.9 ± 47.4	1457.4 ± 55.6	22.6 ± 5.8	−1.2
8	−61.2 ± 17.8	11.0 ± 0.2	5	−40.1 ± 9.1	−414.0 ± 46.4	442.7 ± 19.1	1188.9 ± 117.1	17.4 ± 4.9	−0.8
7	−57.3 ± 7.5	2.4 ± 0.2	5	−38.1 ± 6.2	−471.4 ± 21.3	509.1 ± 40.5	1238.2 ± 162.5	24.1 ± 8.3	−0.5
4	−48.5 ± 4.2	12.1 ± 0.0	7	−38.4 ± 1.7	−379.6 ± 30.2	487.4 ± 18.6	1190.6 ± 72.6	17.1 ± 6.6	0.0

† The final 80 structures were clustered based on the pairwise r.m.s.d. matrix using a 3.5 Å cutoff. The statistics are for the ten lowest energy structures. ‡ The *HADDOCK* score was calculated as the sum $E_{vdw} + E_{elec} + E_{AIR} + E_{desolv}$. § Overall backbone r.m.s.d. from the lowest energy structure. ¶ Number of structures in a given cluster. †† Intermolecular energies (kcal mol^{-1}) were calculated with the OPLS parameters using an 8.5 Å cutoff. ‡‡ *HADDOCK* ambiguous interaction restraint energy (kcal mol^{-1}). §§ Buried surface area (Å^2). ¶¶ Desolvation energy (kcal mol^{-1}). ††† The *Z*-score indicates the standard deviations from the average of a particular cluster in terms of *HADDOCK* score.

Ser576) and two parallel β-strands (β1, Leu521–Met523; β2, Val567–Val569) arranged in the order α1–β1–α2–α3–β2–α4 (Figs. 1*a* and 1*b*). The C-terminal residues after Tyr585 of the crystal structure of the Bt-Lon α subdomain are missing owing to its high flexibility and no electron density was observed. The surface-charge distribution of the crystal structure reveals that most of the charged residues are exposed to the aqueous phase. Several positively charged clusters are clearly observed (Figs. 1*c* and 1*d*).

Co-crystallization of protein and DNA was performed to attempt to understand how the α subdomain recognizes DNA; however, there was no evidence of bound DNA in the solved crystal structure. Therefore, an NMR perturbation experiment was performed to probe the interface of the protein bound to DNA. After heteronuclear three-dimensional NMR spectra of the Bt-Lon α subdomain had been obtained, chemical shift assignment was achieved using a standard procedure (Brünger *et al.*, 1998). The NMR resonances of all backbone ^{15}N, ^{1}H^{N}, ^{1}H$^{\alpha}$, ^{13}C$^{\alpha}$, ^{13}C$'$ and side-chain ^{1}H$^{\beta}$ and ^{13}C$^{\beta}$ atoms were almost completely assigned and deposited in the Biological Magnetic Resonance Data Bank (BMRB accession No. 18652). The secondary structure of the Bt-Lon α subdomain in solution, as deduced from the consensus chemical shift index (CSI), is almost identical to that of the crystal structure. For further NMR study of the protein–DNA complex, we initially acquired two-dimensional ^{1}H–^{15}N HSQC spectra for the α subdomain in complex with various concentrations of the double-stranded DNA ds-ms1, the sequence of which was identified as a hairpin DNA (hp-ms1) as previously reported (Lin *et al.*, 2009). However, the chemical shift perturbations could not clearly be observed as the sample severely precipitated in a condition containing only 0.1 *M* NaCl. The lower affinity ds-ms2 DNA, with 50% identity to ds-ms1, was then used in an NMR titration experiment (Supplementary Fig. S3). On comparison, the trend in chemical shift changes for the two 12-mer duplex DNA fragments is interestingly nearly identical. A selected region of the ^{1}H–^{15}N HSQC spectrum is shown in Fig. 2(*a*). The changes in the DNA binding-induced chemical shift, Δp.p.m., were calculated using the equation $[(\Delta\delta H_N)^2 + (0.2\Delta\delta N)^2]^{1/2}$, where δH_N is the chemical shift change of the amide proton and δN is the chemical shift change of the amide ^{15}N (Fig. 2*b*). The residues with significant chemical-shift changes ($\Delta\delta > 0.05$ p.p.m.) are clustered around α3 (Val541, Arg553 and Lys554), α4 (Thr573, Val574 and Glu575) and β2 (Arg566, Val567 and Thr570), as well as the loop between α1 and β1 (Met511, His514 and Gly517). Accordingly, the disappearance of the HSQC cross-peaks for Glu547, Arg557 and Val560 in the α3 helix is likely to arise from direct binding to DNA. A surface representation of the Bt-Lon α subdomain displaying the shift changes is shown in the inset in Fig. 2(*b*). Of note, the dramatic shift changes of Thr596 and Arg597 are located on the missing linker residues, indicating a possible induced domain–domain conformational change on the addition of DNA.

For docking of the Bt-Lon α subdomain to DNA, ambiguous interaction restraints (AIRs) were generated based on the chemical shift perturbation data in conjugation with the coordinate files of protein and DNA. According to the criteria of *HADDOCK* (Dominguez *et al.*, 2003), the 'active' residues are those that have been shown by mutation to abolish or perturb complex formation and are solvent-exposed. The surrounding residues were chosen as 'passive' residues. After the semi-flexible simulated-annealing and explicit water refinement protocol, the final 80 structures were clustered based on the pairwise r.m.s.d. matrix using a 3.5 Å cutoff and resulted in 12 different clusters. Table 2 shows the statistics of the top five clusters based on the averaged *HADDOCK* score of their top ten structures. Out of the five clusters generated, cluster 1 comprised of 16 structures with a pairwise lowest r.m.s.d. value of 0.9 Å, compared with an r.m.s.d. of 11.5 Å for the second most populated cluster 10 with four structures. Owing to the lower buried surface area of 1457.4 Å^2 and the higher *HADDOCK* score value of −67.7 for cluster 10, it was evident that cluster 1 should be selected for further analysis and to represent the model of the α subdomain–DNA complex. Intriguingly, the *HADDOCK* structure reveals that the α4 helix participates in DNA binding with an optimal orientation onto the major groove (Figs. 2*c* and 2*d*). Three signal-disappeared residues (Glu547, Arg557 and Val560) are all located on the DNA-binding side. In addition, positively charged residues surrounding Arg557, which was positioned on the C-terminus of α3 helix, seem to present a cluster pitch for DNA binding (Figs. 2*e* and 2*f*). The result implies that electrostatic forces may mediate the interactions between the α subdomain and DNA. Furthermore, a DAPI replacement experiment (Supplementary Fig. S4) also provided evidence for DNA major-groove binding of the α subdomain, which is consistent with the docking result.

Table 3
Characterization of the Bt-Lon mutants.

	Peptidase (mean ± SD)†‡				
	−ATP	+ATP (1 m*M*)	ATPase (mean ± SD)†§	T_m (°C)	Fluorescence maximum (nm)
Wild type	65 ± 3.3	695 ± 35.0	1.90 ± 0.10	71.5	338
R98A	75 ± 3.7	750 ± 37.5	2.10 ± 0.10	70.5	338
R370A	67 ± 3.4	800 ± 40.0	2.14 ± 0.11	70.0	338
R518A	72 ± 3.6	845 ± 42.2	2.13 ± 0.11	72.0	339
R557A	72 ± 3.6	755 ± 37.8	2.14 ± 0.11	71.5	339
R566A	73 ± 3.7	740 ± 37.0	2.16 ± 0.12	71.5	339
R590A	86 ± 4.3	815 ± 40.8	2.18 ± 0.11	71.5	338
R697A	64 ± 3.2	665 ± 33.2	1.85 ± 0.10	71.5	338

† The results shown represent the average of at least three separate experiments. ‡ The units are picomoles of Glt-AAF-MNA per microgram of Bt-Lon per hour. § The units are picomoles of inorganic phosphate per microgram of Bt-Lon per hour × 10^{-4}.

3.2. Electrostatic interactions contributed by the Arg518, Arg557 and Arg566 residues in the α subdomain are important for DNA binding by Bt-Lon

From the docking model of the α subdomain in complex with DNA, we proposed that electrostatic interactions play important roles in protein–DNA interaction. To address this issue, we examined the effect of electrostatic interactions on the DNA-binding ability of Bt-Lon. Seven arginine-to-alanine mutants, R98A, R370A, R518A, R557A, R566A, R590A and R697A, were created. Arg98 is located in the N-terminal domain, Arg697 in the protease domain, Arg370 in the α/β subdomain and Arg518, Arg557, Arg566 and Arg590 in the α subdomain of the AAA^+ module. Bt-Lon and the seven mutants were expressed as soluble proteins in *E. coli* BL21(DE3) cells and were purified to about 95% purity as judged by SDS–PAGE (Supplementary Fig. S5*a*). The secondary structure and overall structural integrity of the mutants were similar to those of the wild type according to far-UV CD spectroscopy and intrinsic tryptophan (Trp) fluorescence analysis, respectively (Supplementary Fig. S5*b* and Table 3). In addition, the temperature-unfolding profiles of the mutants were almost identical to the profile of the wild type, which showed a similar melting temperature (T_m) of 71.5°C (Table 3). These results indicate that these seven mutations have no significant effect on the global conformation or structural integrity of the proteins. Furthermore, the catalytic activities, including the peptidase and ATPase activities, of the wild-type and arginine mutants were comparable in both the absence and the presence of ATP (Table 3). Taken together, these data suggest that there are no significant defects in the conformation and catalytic function of the arginine mutants.

Subsequently, we first examined the DNA-binding ability of the arginine mutants using an electrophoretic mobility-shift assay (EMSA). We found that the DNA-binding ability of the R518A, R557A and R566A mutants was largely reduced compared with that of the wild type. However, the R98A, R370A, R590A and R697A mutants showed similar migration profiles to that of the wild type (Supplementary Fig. S6*a*). We further confirmed the DNA-binding ability of the mutants by intrinsic Trp fluorescence spectroscopy. Compared with the wild type, the R518A, R557A and R566A mutants had a lower fluorescence quenching effect on DNA addition (Supplementary Fig. S6*b*, left panel), whereas the R98A, R370A, R590A and R697A mutants exhibited almost the same extent of fluorescence quenching in the presence of DNA (Supplementary Fig. S6*b*, right panel). These results indicate that Arg518, Arg557 and Arg566 located in the α subdomain are crucial for the DNA-binding ability of Bt-Lon. Consistently, these three Arg residues are included in the four clusters of changed residues according to the chemical-shift perturbation experiment (Fig. 2*b*).

3.3. The electrostatic interactions contributed by arginine residues in the AAA^+ module are important for the DNA-stimulated enzymatic activities of Bt-Lon

To better understand the roles of DNA binding by the α subdomain in the regulation of Bt-Lon activity, we examined the peptidase and ATPase activities of seven arginine mutants in the presence of DNA. It has previously been reported that the protease activity of *E. coli* Lon is stimulated by DNA in a dose-dependent manner, but that a high concentration of DNA inhibits proteolysis and ATP hydrolysis (Charette *et al.*, 1984; Chung & Goldberg, 1982). Thus, we first determined whether this finding was also observed in Bt-Lon. We found that little FITC-casein hydrolysis was observed in the absence of ATP and that hydrolysis by Bt-Lon was markedly stimulated by DNA in the presence of ATP (Fig. 3*a*), suggesting that ATP is a prerequisite for the DNA-stimulated proteolytic activity of Bt-Lon. Moreover, in the presence of ATP the proteolytic activity of Bt-Lon was augmented to a plateau at about 8 μg ml^{-1} by an increasing concentration of DNA (Fig. 3*a*). The optimal DNA concentration was used in the following DNA-stimulation experiments. We found that the protease activity of wild-type Bt-Lon was stimulated by DNA and increased to about 1.5-fold (Fig. 3*b*). The DNA-mediated stimulation of the proteolytic activity of arginine mutants in the AAA^+ module (R370A, R518A, R557A, R566A and R590A) was significantly reduced (Fig. 3*b*), suggesting that the electrostatic interactions contributed by the arginine residues in the AAA^+ module are important for the DNA-stimulated proteolytic activity of Bt-Lon. These findings suggest that the electrostatic forces contributed by the arginine residues are responsible not only for the DNA binding of the α subdomain but also for the allosteric regulation by the AAA^+ module of Bt-Lon. Intriguingly, the R557A mutant did not efficiently inhibit DNA-mediated stimulation like the other two arginine mutants in the α subdomain (R518A and R566A), all of which are defective in DNA binding (Supplementary Fig. S6*b*). These findings led to the hypothesis that Arg557 is involved in DNA binding by acting as a switch to negatively regulate activation of the adjacent ATPase domain. To prove this, we examined DNA-mediated stimulation of the ATPase activity of arginine mutants. We consistently observed that arginine mutants in the α subdomain (R518A, R566A and R590A) failed to significantly activate the ATPase activity in the presence of DNA (Fig. 3*c*), confirming that the electrostatic forces contributed by arginine residues are responsible for

allosteric regulation by the AAA$^+$ module of Bt-Lon. Indeed, we found that R557A, which is defective in direct DNA binding, still efficiently stimulates the ATPase activity in the presence of DNA, suggesting a model in which DNA binding to Arg557 in the α subdomain affects ATP entry or binding to an adjacent ATPase module.

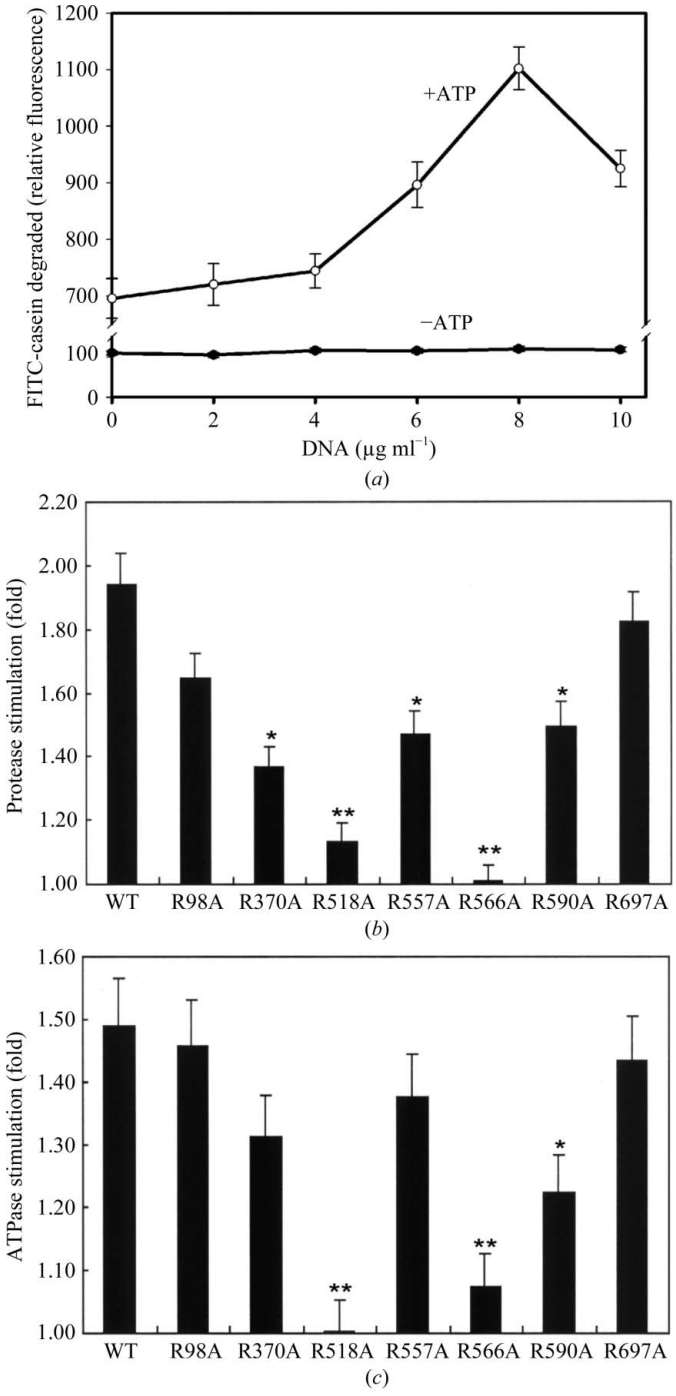

Figure 3
Stimulation of the enzymatic activities of Bt-Lon arginine mutants by DNA. (*a*) The protease activity of Bt-Lon is stimulated by DNA. The stimulation of protease activity by DNA was assayed under various conditions. Increasing concentrations of DNA were incubated with Bt-Lon (0.02 mg ml^{-1}) and FITC-casein (10 μg) in a final volume of 200 μl 50 m*M* Tris–HCl pH 8.0, 150 m*M* NaCl, 10 m*M* $MgCl_2$ and in the presence (empty circles) or the absence (filled circles) of 1.0 m*M* ATP. The rate of FITC-casein hydrolysis was determined. Assays of peptidase (*b*) and ATPase (*c*) activity were performed in the presence or the absence of 8 μg ml^{-1} plasmid DNA. The stimulation of the activities in the absence of DNA was set to 1.

3.4. The electrostatic interactions contributed by arginine residues in the AAA$^+$ module are important for the substrate-stimulated enzymatic activities of Bt-Lon

To explore whether the electrostatic forces contributed by the arginine residues in the AAA$^+$ module are responsible for the allosteric regulation of Bt-Lon, we investigated the stimulatory effect on the enzymatic activities of the mutants by the substrate. As shown in Fig. 4, α-casein stimulated both the peptidase and the ATPase activities of wild-type Bt-Lon. The stimulation of the peptidase and ATPase activities by α-casein in the R370A, R518A, R557A, R566A and R590A mutants was significantly reduced compared with the wild type (Figs. 4*a* and 4*b*), suggesting that the arginine residues in the AAA$^+$ module are important for the substrate-stimulated enzymatic activities of Bt-Lon. This result is consistent with previous studies that have suggested that communication between the

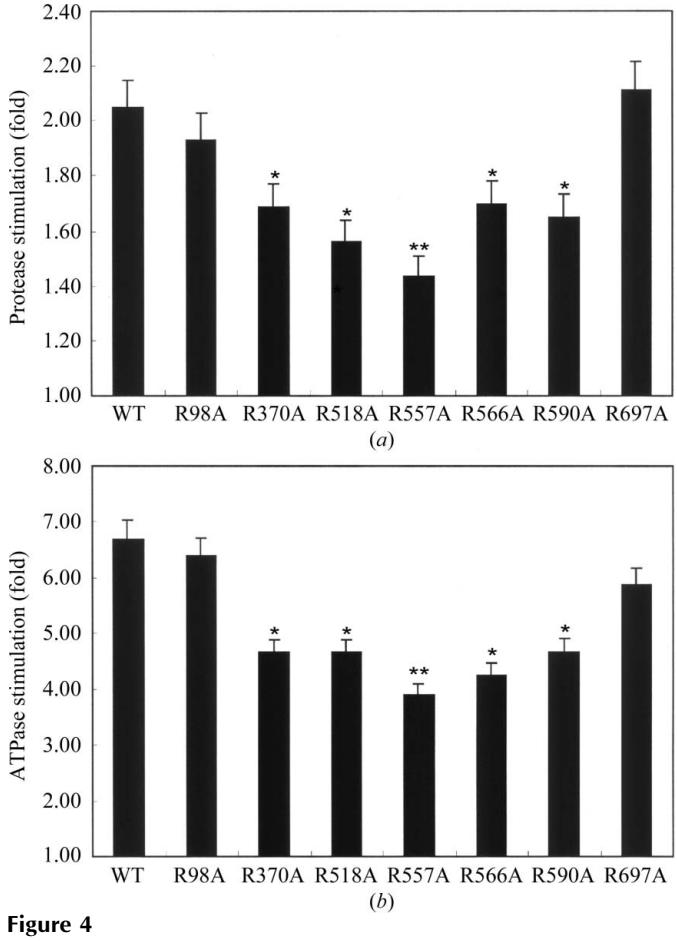

Figure 4
Electrostatic interactions contributed by the arginine residues in the AAA$^+$ module are important to the allosteric stimulation of the activities of Bt-Lon by the substrate. The peptidase (*a*) or ATPase (*b*) activities of the Bt-Lon mutants were stimulated by α-casein. The reaction conditions were identical to those in Fig. 4 except that the DNA was replaced by 8 μg ml^{-1} α-casein.

AAA$^+$ module and the protease domain is important for the catalytic activity of Lon (Fischer & Glockshuber, 1994; Starkova *et al.*, 1998). More intriguingly, the R557A mutant showed the greatest reduction in the stimulation of the enzymatic activity by α-casein. Thus, we suggested that Arg557 not only plays an important role in the direct interaction with DNA but also has a putative function in domain–domain communication inside Bt-Lon. In addition, under the same conditions, the stimulation of ATPase by DNA is much lower than that by α-casein (Supplementary Fig. S7). Taken together, the data suggest that the electrostatic interactions contributed by arginine residues in AAA$^+$ play an important role in the allosteric stimulation of Bt-Lon by two allosteric regulators: DNA and protein substrate. Furthermore, our results imply that direct binding to DNA is a negative allosteric regulator of the ATPase activation of Bt-Lon (Fig. 3*c*).

3.5. A low concentration of DNA stimulates ATP-dependent proteolysis and a high concentration of DNA inhibits ATP-binding-induced conformational changes and ATP-mediated proteolysis in Bt-Lon

We speculated that DNA binding to the α subdomain negatively regulates the activation of Bt-Lon ATPase through affecting the conformation of the AAA$^+$ module. This hypothesis is supported by previous studies that have shown that ATP inhibits the DNA-binding ability of human mitochondrial Lon (Liu *et al.*, 2004). However, one study showed that DNA stimulates the ATPase and protease activities of prokaryotic Lon (Chung & Goldberg, 1982). Accordingly, we pre-incubated different amounts of DNA with Bt-Lon before the addition of FITC-casein and ATP and then examined the ATP-dependent protease activity of Bt-Lon. The hydrolysis of FITC-casein was stimulated when 2 μg ml^{-1} DNA was pre-incubated with Bt-Lon. An inhibitory effect on ATP-dependent proteolysis was observed when Bt-Lon was pre-incubated with more than 2 μg ml^{-1} DNA (Fig. 5*a*). This result suggests that the prior binding of a low level of DNA stimulates ATP-mediated proteolysis of Bt-Lon, but the binding of a high level of DNA by Bt-Lon may induce a change in conformation that is not favoured to stimulate ATP hydrolysis. To prove this hypothesis, we performed order-of-addition experiments to compare the effect of the addition of DNA followed by ATP or the reverse order on the conformational change of Bt-Lon using Trp fluorescence. We first found an optimal condition in which 1 m*M* of ATP, a saturating condition (Patterson *et al.*, 2004), caused the same conformational change of Bt-Lon as was caused by 100 μg ml^{-1} DNA for the

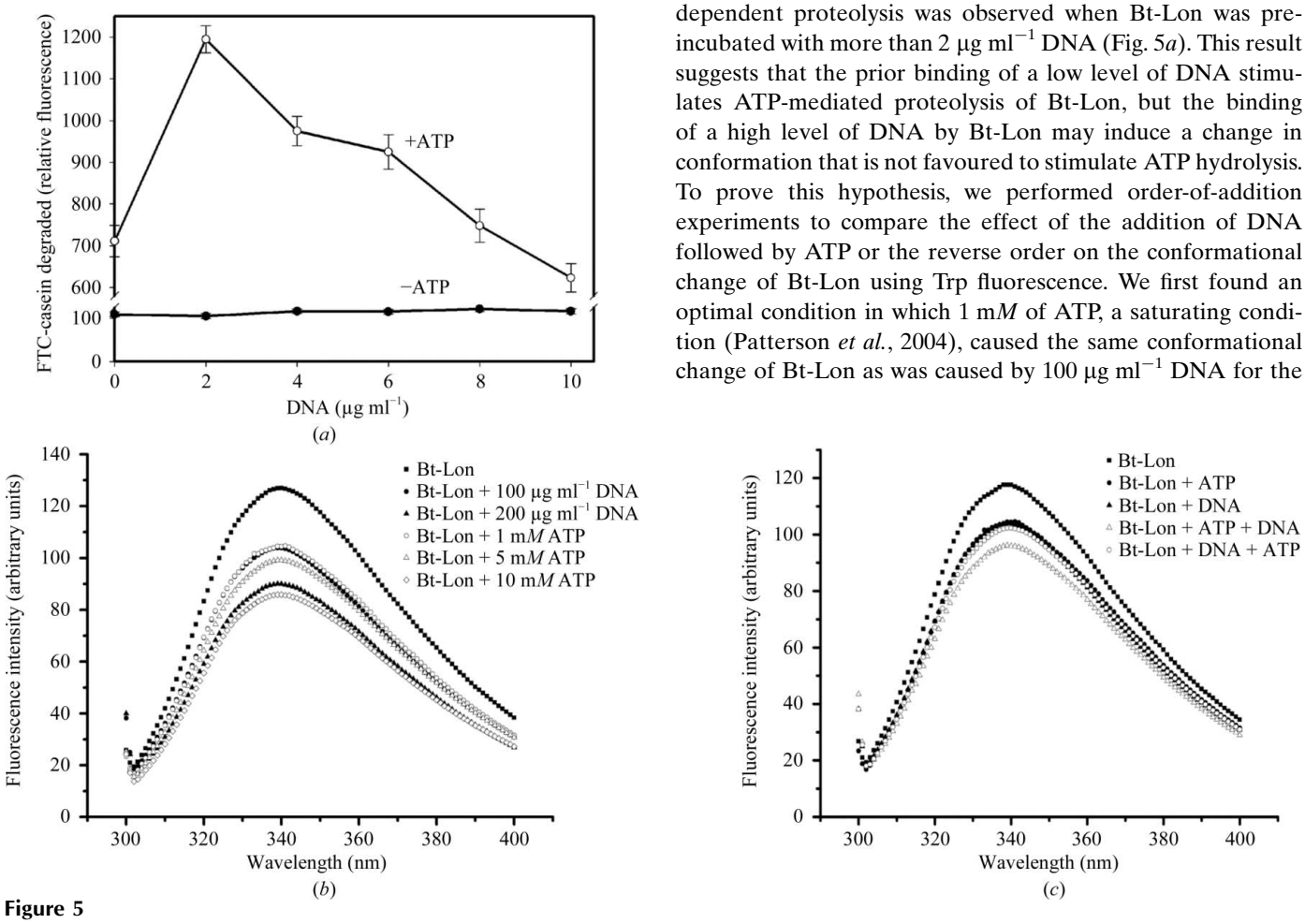

Figure 5
The effect of DNA concentration on the proteolytic activity and ATP-binding-induced conformational changes of Bt-Lon. (*a*) The protease activity of Bt-Lon is regulated by pre-incubated DNA. The stimulation of protease activity by pre-incubated DNA was assayed under various conditions. Increasing concentrations of DNA were pre-incubated with Bt-Lon (0.02 mg ml^{-1}) for 10 min at room temperature before the addition of ATP and FITC-casein (10 μg) in a final volume of 200 μl 50 m*M* Tris–HCl pH 8.0, 150 m*M* NaCl, 10 m*M* $MgCl_2$ and in the presence (empty circles) or the absence (filled circles) of 1.0 m*M* ATP. The rate of FITC-casein hydrolysis was determined. (*b*) Characterization of quenching of the intrinsic tryptophan fluorescence spectra of Bt-Lon by various concentrations of DNA or ATP. The intrinsic fluorescence emission spectra of Bt-Lon (0.2 mg ml^{-1}) in the absence and presence of the indicated concentrations of DNA or ATP were recorded at 25°C. (*c*) The ATP-binding-induced conformational changes in Bt-Lon are inhibited by a high concentration of pre-incubated DNA as shown by intrinsic tryptophan fluorescence. The intrinsic fluorescence emission spectra of Bt-Lon (0.2 mg ml^{-1}) in the presence and absence of ATP and/or DNA were recorded at 25°C. The order-of-addition experiment was also performed by either pre-incubating Bt-Lon with plasmid DNA (100 μg ml^{-1}) for 10 min and then adding ATP (1 m*M*) (empty circles) or pre-incubating Bt-Lon with ATP for 5 min and then adding plasmid DNA (empty triangles).

order-of-addition experiment (Fig. 5*b*). The same ratio of DNA and Bt-Lon (100 µg ml^{-1} DNA, 0.2 mg ml^{-1} Bt-Lon) was used as in Fig. 5(*a*). Fig. 5(*c*) consistently shows that the addition of DNA or ATP alone causes a similar decrease in the intrinsic fluorescent content of Bt-Lon. However, when DNA was added first the subsequent conformational changes on ATP binding were inhibited, whereas when ATP was added first the subsequent addition of DNA was still able to cause a further conformational change in Bt-Lon (Fig. 5*c*). These observations confirm that the prior binding of a high level of DNA to Bt-Lon prevents ATP-binding-induced conformational changes in Bt-Lon and inhibits the ATP-mediated proteolysis of Bt-Lon.

4. Discussion

Lon is a DNA-binding protease and its catalytic activities are regulated by DNA and the protein substrate. However, little is known about the mechanism of DNA binding and DNA-mediated allosteric regulation of Lon protease. Here, we solved the crystal structure of the α subdomain of the AAA$^+$ module of Bt-Lon, which is involved in DNA binding. The structure shows a surface of highly positive charge, including Arg518, Arg566 and Arg557. NMR perturbation and a *HADDOCK* model also showed that the three arginine residues in the α subdomain are important for interaction with duplex DNA. We further investigated the roles of the arginine residues in the AAA$^+$ module in DNA binding and in DNA-mediated allosteric regulation. In addition, how DNA binding regulates the catalytic activities of Bt-Lon through the regulation of tertiary and quaternary structure was studied.

We suggest that electrostatic interactions play important roles in the Bt-Lon–DNA interaction. Protein–DNA interactions can be either sequence-specific or nonspecific. Nonspecific recognition involves purely electrostatic interactions between the negatively charged phosphates of the sugar-phosphate backbones and the basic residues (Arg, Lys, and His) that surround the binding sites of the protein (Kalodimos *et al.*, 2004; Ucci & Cole, 2004). In addition, electrostatic interactions contributed by arginine residues in the AAA$^+$ module are responsible not only for the DNA binding of the α subdomain but also for allosteric regulation by DNA and the protein substrate in Bt-Lon. Since DNA allosterically stimulates the enzymatic activities of Bt-Lon, the reduced affinity for DNA in the R518A, R557A and R566A mutants would be expected to influence the DNA-mediated allosteric stimulation of enzymatic activity. Indeed, DNA failed to stimulate the peptidase and ATPase activities of the R518A and R566A mutants (Figs. 3*b* and 3*c*). Unexpectedly, the ATPase activity of R557A was still considerably stimulated by DNA (Fig. 3*c*). To gain insight into detailed structural information, a truncated Bt-Lon structure (Fig. 6*a*) was constructed by homology modelling using a fragment (250–774) of *B. subtilis* Lon (Bs-Lon) as a template. Superposition of the α subdomain–DNA complex model and the Bt-Lon monomer revealed that DNA bound to the α subdomain may cause a slight domain rearrangement *via* a perturbing link region, as shown by our chemical shift perturbation data (Fig. 6*b*). In addition, DNA-mediated allosteric regulation may be stimulated to affect the neighbouring monomer by the α subdomain or its bound

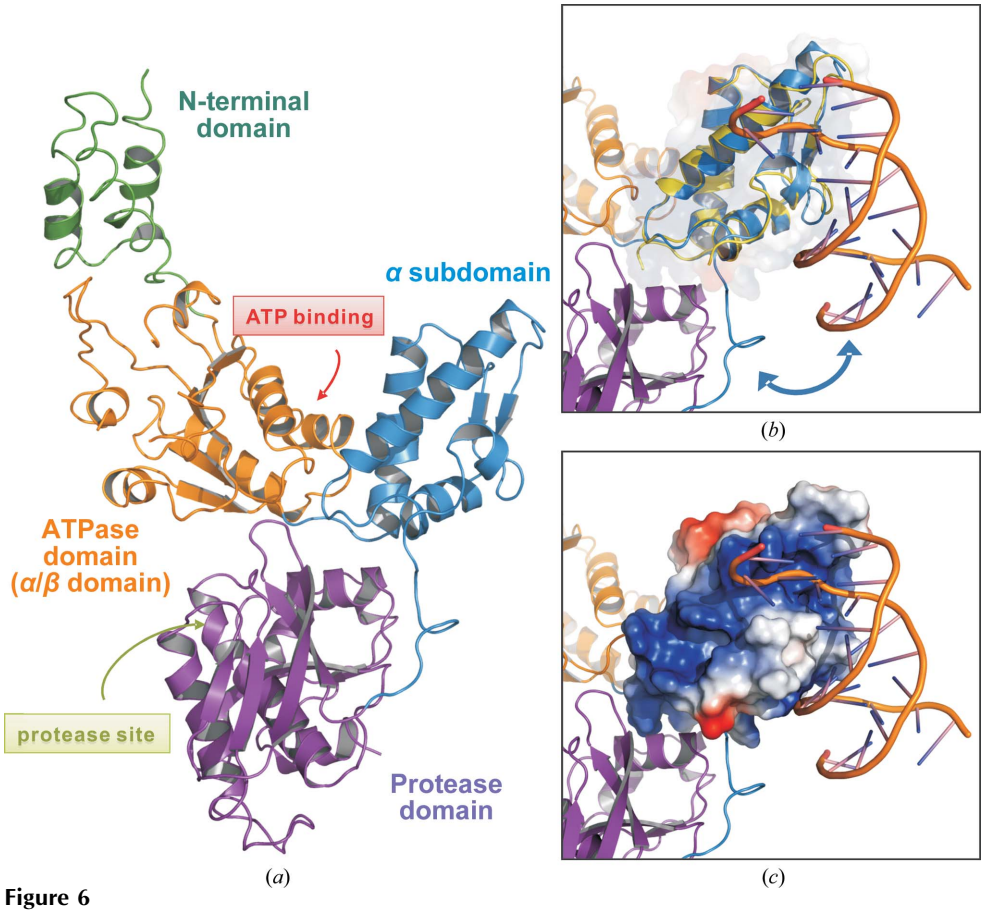

Figure 6
Model of Lon protease bound to DNA to examine the functional implications. (*a*) Homology model of the Bt-Lon monomer derived from the crystal structure of Bs-Lon. Each domain is shown in a different colour. ATP-binding and protease catalytic regions are indicated by arrows. (*b*) Superposition of the α subdomain with the bound DNA model (yellow) and the Bt-Lon monomer (blue) reveals that DNA bound to the Bt-Lon α subdomain may cause a slight domain rearrangement *via* a perturbing link region as shown by our chemical-shift perturbation data. (*c*) A surface-charged representation of the α subdomain is shown. The DNA-mediated allosteric regulation may be stimulated to affect the neighbouring monomer by the α subdomain or its bound DNA.

DNA (Fig. 6*c*). On the other hand, we also showed that the electrostatic interactions contributed by the arginine residues in the AAA^+ module, including Arg557, play important roles in α-casein-mediated allosteric stimulation (Fig. 4). These results suggested that Arg557 in the α subdomain plays a dual role in the regulation of ATPase by direct DNA binding and in domain–domain communication in Bt-Lon. Previous studies have suggested that the α-casein binding site is in the N-terminal domain (Lee, Hsu *et al.*, 2004; Roudiak & Shrader, 1998; Rudyak & Shrader, 2000), which has been termed the allosteric site (Goldberg, 1992; Maurizi, 1992). Once α-casein binds to the enzyme, the N-terminal domain undergoes changes in conformation and orientation. Transduction of the mechanical motions within the N-terminal domain when substrate is bound provides the driving force for various functions, including ATP/ADP exchange and the translocation of proteins to a linked protease domain (Licht & Lee, 2008). Consequentially, conformational changes in the AAA^+ module may affect subunit interfaces within the protease domain through the α subdomain (Botos *et al.*, 2004). The results presented here support the hypothesis that electrostatic interactions contributed by arginine residues in the AAA^+ module play highly crucial roles in domain–domain communication in the allosteric regulation of Bt-Lon.

The relationship between DNA binding and the enzymatic activities of prokaryotic Lon remains unclear (Lee & Suzuki, 2008). In the present report, we suggest that electrostatic interactions contributed by the arginine residues Arg518, Arg557 and Arg566 in the α subdomain play an important role in DNA interaction and allosteric stimulation by two allosteric regulators: DNA and the protein substrate. However, the electrostatic interaction contributed by Arg557 that directly binds to DNA is a negative allosteric regulator of the stimulation of the Bt-Lon ATPase. Further studies found that a low concentration of DNA stimulates ATP-dependent proteolysis and a high concentration of DNA inhibits ATP-binding-induced conformational changes and ATP-mediated proteolysis of Bt-Lon (Fig. 5). We consistently found that under the same conditions DNA stimulates ATPase activity more ineffectively than α-casein (Supplementary Fig. S7). Our observations are consistent with several lines of evidence. Chung & Goldberg (1982) reported that plasmid DNA increases the binding affinity of casein but does not increase that of ATP. Charette *et al.* (1984) reported that a high concentration of DNA significantly inhibits the ATP-dependent protease activity.

From a physiological viewpoint, the binding of a high level of DNA prior to other regulators means that Lon protease originally localizes on the chromosomal DNA and its activity is inhibited through inhibiting ATP-binding-induced conformational changes. When the protease interacts with its substrate and ATP on the DNA, its DNA-binding affinity is reduced but the DNA still stabilizes the overall oligomeric structure, its oligomerization is promoted and its activity is activated, and the protease efficiently degrades its substrate (Kalodimos *et al.*, 2004). Our model is supported by the following findings. A recent report suggested that human mitochondrial Lon is a component of mitochondrial nucleoids in which it degrades or processes proteins involved in DNA metabolism and replication (Liu *et al.*, 2004). In addition, an excess of free Lon is unfavourable and lethal to cells under normal conditions (Goff & Goldberg, 1987). In conclusion, we provide the structural and biochemical bases for studies that will define the critical roles of its DNA-binding activity in the regulation of the catalytic activities of Lon. Further investigations are required to clarify the role of the DNA-binding ability of Lon *in vivo* and whether different functional states or oligomeric forms of Lon have different affinities for DNA.

We would like to thank the Technology Commons of the College of Life Science and Center for Systems Biology, National Taiwan University for instrumental support in protein crystallization. Portions of this research were carried out on beamlines BL13B1 and BL13C1 of the National Synchrotron Radiation Research Center, Taiwan. The NMR spectra were obtained at the NMR Facility of Instrumentation Center in NTU and the High-Field Nuclear Magnetic Resonance Center (HF-NMRC), Taiwan. This work was supported financially by the National Science Council (NSC 102-2627-M-400-001 to A-YL, NSC 96-2311-B-001-010 to S-HW and NSC 99-2119-M-002-010 to C-HH), National Taiwan University (NTU-ERP-101R8600-1 and NTU-ICRP-102R7560-5 to C-HH) and National Health Research Institutes (102A1-CA-PP-08 to A-YL) in Taiwan.

References

Adams, P. D. *et al.* (2010). *Acta Cryst.* D**66**, 213–221.
Alexandre, J., Hu, Y., Lu, W., Pelicano, H. & Huang, P. (2007). *Cancer Res.* **67**, 3512–3517.
Botos, I., Melnikov, E. E., Cherry, S., Khalatova, A. G., Rasulova, F. S., Tropea, J. E., Maurizi, M. R., Rotanova, T. V., Gustchina, A. & Wlodawer, A. (2004). *J. Struct. Biol.* **146**, 113–122.
Bradford, M. M. (1976). *Anal. Biochem.* **72**, 248–254.
Brünger, A. T., Adams, P. D., Clore, G. M., DeLano, W. L., Gros, P., Grosse-Kunstleve, R. W., Jiang, J.-S., Kuszewski, J., Nilges, M., Pannu, N. S., Read, R. J., Rice, L. M., Simonson, T. & Warren, G. L. (1998). *Acta Cryst.* D**54**, 905–921.
Charette, M. F., Henderson, G. W., Doane, L. L. & Markovitz, A. (1984). *J. Bacteriol.* **158**, 195–201.
Chen, S.-H., Suzuki, C. K. & Wu, S.-H. (2008). *Nucleic Acids Res.* **36**, 1273–1287.
Chen, Y.-D., Chang, Y.-Y., Wu, S.-H. & Hsu, C.-H. (2013). *Acta Cryst.* F**69**, 899–901.
Chen, Y.-D., Wu, S.-H. & Hsu, C.-H. (2013). *Biomol. NMR Assign.*, doi:10.1007/s12104-013-9490-6.
Cheng, C.-W., Kuo, C.-Y., Fan, C.-C., Fang, W.-C., Jiang, S. S., Lo, Y.-K., Wang, T.-Y., Kao, M.-C. & Lee, A. Y.-L. (2013). *Cell Death Dis.* **4**, e681.
Chung, C. H. & Goldberg, A. L. (1981). *Proc. Natl Acad. Sci. USA*, **78**, 4931–4935.
Chung, C. H. & Goldberg, A. L. (1982). *Proc. Natl Acad. Sci. USA*, **79**, 795–799.
Delaglio, F., Grzesiek, S., Vuister, G. W., Zhu, G., Pfeifer, J. & Bax, A. (1995). *J. Biomol. NMR*, **6**, 277–293.
Dijk, M. van, van Dijk, A. D., Hsu, V., Boelens, R. & Bonvin, A. M. (2006). *Nucleic Acids Res.* **34**, 3317–3325.
Dominguez, C., Boelens, R. & Bonvin, A. M. (2003). *J. Am. Chem. Soc.* **125**, 1731–1737.
Duman, R. E. & Löwe, J. (2010). *J. Mol. Biol.* **401**, 653–670.

Dyck, L. van, Neupert, W. & Langer, T. (1998). *Genes Dev.* **12**, 1515–1524.
Dyck, L. van, Pearce, D. A. & Sherman, F. (1994). *J. Biol. Chem.* **269**, 238–242.
Emsley, P. & Cowtan, K. (2004). *Acta Cryst.* D**60**, 2126–2132.
Eswar, N., Eramian, D., Webb, B., Shen, M.-Y. & Sali, A. (2008). *Methods Mol. Biol.* **426**, 145–159.
Fischer, H. & Glockshuber, R. (1994). *FEBS Lett.* **356**, 101–103.
Fu, G. K. & Markovitz, D. M. (1998). *Biochemistry*, **37**, 1905–1909.
Fu, G. K., Smith, M. J. & Markovitz, D. M. (1997). *J. Biol. Chem.* **272**, 534–538.
Fukui, T., Eguchi, T., Atomi, H. & Imanaka, T. (2002). *J. Bacteriol.* **184**, 3689–3698.
Gill, R. E., Karlok, M. & Benton, D. (1993). *J. Bacteriol.* **175**, 4538–4544.
Gillette, T. G., Gonzalez, F., Delahodde, A., Johnston, S. A. & Kodadek, T. (2004). *Proc. Natl Acad. Sci. USA*, **101**, 5904–5909.
Goff, S. A. & Goldberg, A. L. (1987). *J. Biol. Chem.* **262**, 4508–4515.
Goldberg, A. L. (1992). *Eur. J. Biochem.* **203**, 9–23.
Goldberg, A. L., Moerschell, R. P., Chung, C. H. & Maurizi, M. R. (1994). *Methods Enzymol.* **244**, 350–375.
Gonzalez, F., Delahodde, A., Kodadek, T. & Johnston, S. A. (2002). *Science*, **296**, 548–550.
Gottesman, S. (1996). *Annu. Rev. Genet.* **30**, 465–506.
Gottesman, S. & Maurizi, M. R. (1992). *Microbiol. Rev.* **56**, 592–621.
He, G.-P., Muise, A., Li, A. W. & Ro, H.-S. (1995). *Nature (London)*, **378**, 92–96.
Hsu, C.-H., Liao, Y.-D., Pan, Y.-R., Chen, L.-W., Wu, S.-H., Leu, Y.-J. & Chen, C. (2003). *J. Mol. Biol.* **326**, 1189–1201.
Hsu, C.-H. & Wang, A. H.-J. (2011). *Nucleic Acids Res.* **39**, 6764–6774.
Hubbard, S. J. & Thornton, J. M. (1993). *NACCESS*. Department of Biochemistry and Molecular Biology, University College London, England.
Kalodimos, C. G., Biris, N., Bonvin, A. M., Levandoski, M. M., Guennuegues, M., Boelens, R. & Kaptein, R. (2004). *Science*, **305**, 386–389.
Ladokhin, A. S. (2000). *Encyclopedia of Analytical Chemistry*, edited by R. A. Meyers, pp. 5762–5779. Chichester: John Wiley & Sons.
Lanzetta, P. A., Alvarez, L. J., Reinach, P. S. & Candia, O. A. (1979). *Anal. Biochem.* **100**, 95–97.
Lee, A.-Y., Hsu, C.-H. & Wu, S.-H. (2004). *J. Biol. Chem.* **279**, 34903–34912.
Lee, I. & Suzuki, C. K. (2008). *Biochim. Biophys. Acta*, **1784**, 727–735.
Lee, A.-Y., Tsay, S.-S., Chen, M.-Y. & Wu, S.-H. (2004). *Eur. J. Biochem.* **271**, 834–844.
Licht, S. & Lee, I. (2008). *Biochemistry*, **47**, 3595–3605.
Lin, Y.-C., Lee, H.-C., Wang, I., Hsu, C.-H., Liao, J.-H., Lee, A. Y.-H., Chen, C. & Wu, S.-H. (2009). *Biochem. Biophys. Res. Commun.* **388**, 62–66.
Liu, T., Lu, B., Lee, I., Ondrovicová, G., Kutejová, E. & Suzuki, C. K. (2004). *J. Biol. Chem.* **279**, 13902–13910.
Maurizi, M. R. (1992). *Experientia*, **48**, 178–201.
McCoy, A. J., Grosse-Kunstleve, R. W., Adams, P. D., Winn, M. D., Storoni, L. C. & Read, R. J. (2007). *J. Appl. Cryst.* **40**, 658–674.
Menon, A. S. & Goldberg, A. L. (1987). *J. Biol. Chem.* **262**, 14929–14934.
Mizusawa, S. & Gottesman, S. (1983). *Proc. Natl Acad. Sci. USA*, **80**, 358–362.
Morris, A. L., MacArthur, M. W., Hutchinson, E. G. & Thornton, J. M. (1992). *Proteins*, **12**, 345–364.
Murshudov, G. N., Skubák, P., Lebedev, A. A., Pannu, N. S., Steiner, R. A., Nicholls, R. A., Winn, M. D., Long, F. & Vagin, A. A. (2011). *Acta Cryst.* D**67**, 355–367.
Neuwald, A. F., Aravind, L., Spouge, J. L. & Koonin, E. V. (1999). *Genome Res.* **9**, 27–43.
Nomura, K., Kato, J., Takiguchi, N., Ohtake, H. & Kuroda, A. (2004). *J. Biol. Chem.* **279**, 34406–34410.
Otwinowski, Z. & Minor, W. (1997). *Methods Enzymol.* **276**, 307–326.
Pace, C. N. (1990). *Trends Biotechnol.* **8**, 93–98.
Patterson, J., Vineyard, D., Thomas-Wohlever, J., Behshad, R., Burke, M. & Lee, I. (2004). *Biochemistry*, **43**, 7432–7442.
Robertson, G. T., Kovach, M. E., Allen, C. A., Ficht, T. A. & Roop, R. M. II (2000). *Mol. Microbiol.* **35**, 577–588.
Rotanova, T. V., Botos, I., Melnikov, E. E., Rasulova, F., Gustchina, A., Maurizi, M. R. & Wlodawer, A. (2006). *Protein Sci.* **15**, 1815–1828.
Roudiak, S. G. & Shrader, T. E. (1998). *Biochemistry*, **37**, 11255–11263.
Royer, C. A. (1995). *Methods Mol. Biol.* **40**, 65–89.
Rudyak, S. G. & Shrader, T. E. (2000). *Protein Sci.* **9**, 1810–1817.
Sancar, A. & Hearst, J. E. (1993). *Science*, **259**, 1415–1420.
Schmidt, R., Decatur, A. L., Rather, P. N., Moran, C. P. Jr & Losick, R. (1994). *J. Bacteriol.* **176**, 6528–6537.
Sonezaki, S., Okita, K., Oba, T., Ishii, Y., Kondo, A. & Kato, Y. (1995). *Appl. Microbiol. Biotechnol.* **44**, 484–488.
Starkova, N. N., Koroleva, E. P., Rumsh, L. D., Ginodman, L. M. & Rotanova, T. V. (1998). *FEBS Lett.* **422**, 218–220.
Suzuki, C. K., Suda, K., Wang, N. & Schatz, G. (1994). *Science*, **264**, 273–276.
Takaya, A., Tomoyasu, T., Tokumitsu, A., Morioka, M. & Yamamoto, T. (2002). *J. Bacteriol.* **184**, 224–232.
Twining, S. S. (1984). *Anal. Biochem.* **143**, 30–34.
Ucci, J. W. & Cole, J. L. (2004). *Biophys. Chem.* **108**, 127–140.
Vasilyeva, O. V., Kolygo, K. B., Leonova, Y. F., Potapenko, N. A. & Ovchinnikova, T. V. (2002). *FEBS Lett.* **526**, 66–70.
Wang, N., Gottesman, S., Willingham, M. C., Gottesman, M. M. & Maurizi, M. R. (1993). *Proc. Natl Acad. Sci. USA*, **90**, 11247–11251.
Wishart, D. S., Bigam, C. G., Yao, J., Abildgaard, F., Dyson, H. J., Oldfield, E., Markley, J. L. & Sykes, B. D. (1995). *J. Biomol. NMR*, **6**, 135–140.
Zehnbauer, B. A., Foley, E. C., Henderson, G. W. & Markovitz, A. (1981). *Proc. Natl Acad. Sci. USA*, **78**, 2043–2047.
Zheng, W. & Johnston, S. A. (1998). *Mol. Cell. Biol.* **18**, 3580–3585.
Zhu, J. & Winans, S. C. (2001). *Proc. Natl Acad. Sci. USA*, **98**, 1507–1512.